

Structural, morphological and optical properties of nanocrystalline ZnO films deposited by RF sputtering at different bias voltages

R. SUBBA REDDY, A. SIVASANKAR REDDY^a, S. UTHANNA*

Department of Physics, Sri Venkateswara University, Tirupati- 517 502, India

^aDivision of Advanced Materials Engineering, Kongju National University, Budaedong, Cheonan city, South Korea

In the present study high optical transmittance ZnO thin films were deposited by RF magnetron sputtering on p- type (100) silicon and glass substrates by varying the substrate bias voltages ranging from 0 to -120 V. The effect of substrate bias voltage on the structural, morphological and optical properties was studied by using X-ray diffraction, scanning electron microscope, atomic force microscope, and UV-Vis-NIR spectrophotometer. The X-ray diffraction results confirmed that the films consists of ZnO peaks of (100), (002) and (110). The Fourier transform infrared spectrum confirms the presence of Zn-O bonding at wave number of 409 cm⁻¹. The optical transmittance data reveals the average transmittance in the visible range more than 80% for all films. Optical band gap of ZnO films first increased from 3.14 to 3.16 eV and then decreased to 3.10 eV at higher substrate bias voltages.

(Received December 28, 2012; accepted April 11, 2012)

Keywords: Thin Films, Sputtering, ZnO films, Structure, Optical properties

1. Introduction

Zinc oxide is an n-type semiconductor in nature and having a high chemical stability, making it ideal for another potentially efficient short wavelength light emitting material [1]. ZnO is direct transition compound having hexagonal wurtzite structure, a wide energy band gap, great neutral abundance, excellent piezoelectric and optical properties [2]. The high visible transparency of ZnO films helps to use in thin film transistors, UV detectors, UV and blue light emitting and laser diodes [3]. The wide band gap, great neutral abundance and absence of toxicity are a good candidate for short wavelength optoelectronic devices, chemical sensors and solar cells [4]. In the past decade, one-dimensional nanomaterials, such as nanotubes, nanorods, nanobelts and nanowires are attractive considerable attentions because of their peculiar structure characteristics and also wide ranging potential application in nanodevices. In recent years, one-dimensional ZnO nanostructures have been attracted much attention due to their remarkable physical and chemical properties. ZnO nanostructures have been used as photo electrode materials for the fabrication of dye sensitized solar cells (DSSCs), photo detectors, hydrogen storage, chemical and biosensors, photocatalyst [5]. ZnO nanowires are believed to be a good candidate for gas sensing application due to its specific area, fine particle size, and the quantum confinement properties [6]. Nanocrystalline ZnO films have been grown by various deposition techniques such as reactive electron beam evaporation, thermal evaporation, Sol-gel method, Pulsed filtered cathode vacuum arc deposition, Pulsed laser

deposition, Atomic layer deposition technique, Molecular beam epitaxy, DC magnetron sputtering and RF magnetron sputtering [7-15] etc. Among these methods, RF magnetron sputtering is one of the most powerful techniques for the deposition of transparent conducting oxide films due to its simplicity, better reproducibility, and low substrate temperature, good uniformity and good thickness control of the film. In this investigation nanostructure (nanowires) ZnO thin films grown on silicon and glass substrates by using RF magnetron sputtering method and studied the substrate bias voltage influenced structural, morphological and optical properties of the ZnO films.

2. Experimental details

ZnO thin films were deposited on to p- type silicon (100) and glass substrates by RF magnetron sputtering system using Zinc target (99.9% purity). The silicon and Corning glass substrates were thoroughly cleaned with organic solvents and dried before loading the sputtering chamber. The chamber was pumped down to 2×10^{-4} Pa by using diffusion and rotary pump combination. Before deposition of each film, the target was presputtered for 15 min with pure argon in order to remove any contamination on the target surface and the make the system stable and to reach optimum condition. ZnO thin films were deposited at different bias voltages in the range from 0 to -90 V by keeping the other deposition conditions such as oxygen partial pressure, sputtering pressure and sputtering power

as constant. The process parameters fixed during growth of the films are given in Table 1.

Table: 1 Process parameters maintained during the growth of the ZnO films.

Sputter target : (50 mm dia. and 3 mm thick)	
Target to substrate distance	: 50mm
Base pressure	: 2×10^{-4} Pa
Oxygen partial pressure (p_{O_2})	: 2×10^{-2} Pa
Sputter pressure	: 5 Pa
Substrate temperature (T_s)	: 303 K
Bias voltage (V_b)	: 0 -90 V
Deposition time	: 60 min

The deposited thin films thickness was measured by using of α - step profilometer, the crystallographic structure of the films determined with glancing angle X- ray diffraction (XRD) taken on a Bruker D8 Advance Diffractometer at the glancing angle of 4° using monochromatic Co $K\alpha_1$ radiation ($\lambda = 1.78897 \text{ \AA}$). The surface morphology of the films was analyzed by atomic force microscopy (AFM) and Scanning electron microscopy (SEM). Fourier transform infrared spectroscopic (FTIR) measurements in the wave- number range from 400 to 4000 cm^{-1} were carried out using Nicolet Magana IR 750, FTIR spectrophotometer. The optical transmittance of the films was recorded using UV-Vis-NIR Perkin – Elmer double beam spectrophotometer in the wavelength range 300 - 2500 nm.

3. Results and discussions

3.1. Deposition rate

Fig.1 shows the variation of deposition rate with substrate bias voltage. The deposition rate of the films increased from 3.9 to 5.2 nm/min with increasing the substrate bias voltage from 0 to -60 V. The increasing of the deposition rate with bias voltage was due to attracting the positively charged molecules and clusters of the sputtered material in the plasma, which incorporate the sputtered material to arrive on the surface of the substrate. As the bias voltage increased from -60 to -120 V the deposition rate decreased from 5.2 to 3.6 nm/min due to the bombardment makes the molecular re- sputter from the films hence the decrease in the deposition rate. This type of dependence of deposition rate on substrate bias voltage was also observed by Yang et al. [16] in RF magnetron sputtered indium tin oxide thin films. Nirupama et al. [17] also reported that the deposition rate first increased and thereafter decreased at higher substrate bias voltages in DC magnetron sputtered molybdenum oxide thin films.

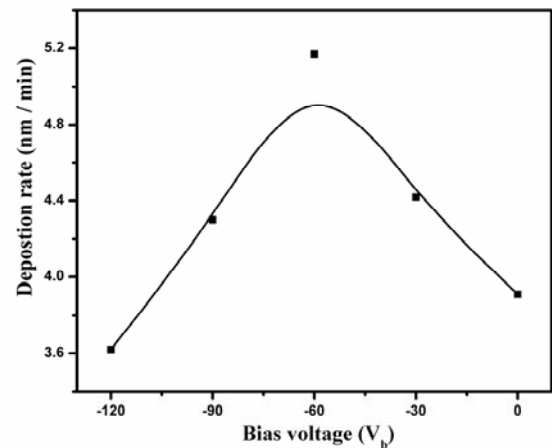


Fig. 1. Variation in deposition rate of ZnO films with substrate bias voltage

3.2. Structural analysis

Fig.2 shows the XRD profiles of ZnO films deposited at different bias voltages ranging from 0 to -90 V. The films formed at zero bias voltage, consist (100) and (110) orientations of polycrystalline ZnO. The films deposited at -30 V the XRD profiles reveals the (100) peak intensity decreases and presence an additional c-axis orientation of (002). When the films formed at bias voltage of -60 V the intensity of (100), (002) peaks increased due to the negative bias

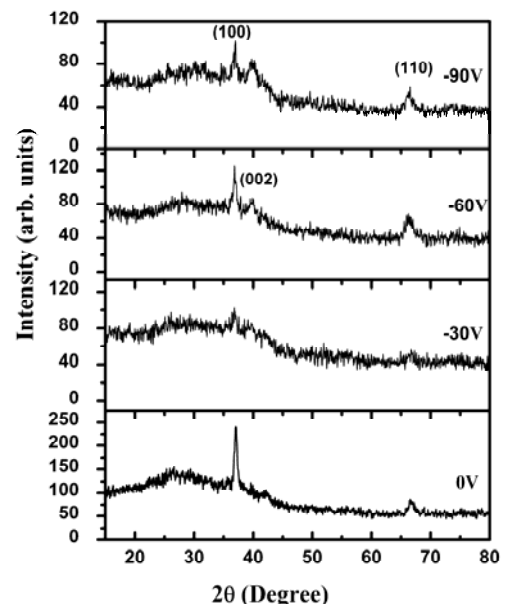


Fig. 2. XRD profiles of ZnO films deposited at various substrate bias voltage.

Voltage provides thermal energy, thereby increasing their local temperature and improvement the crystallinity. The intensity of the (100) and (002) peaks improved at the -60 V bias voltage may be due to the enhancement of energy to the molecules which increase the diffusion mobility of the particles [18]. Further increasing of bias voltage of -90 V, the intensity of (100) and (002) peaks decreased. Ma et al. [19], Flyckyngerova et al. [20] reported the decrease of (002) peak with increase of bias voltage higher than -60 V, with the lower deposition rate and small crystallite size. Such type of results was also found in magnetron sputtered TiO₂ thin films [21]. At higher bias voltage condition ion bombardment during films deposition may be induce a high defeat density in the film and the resputtering.

Fig.3 shows the bias voltage dependence crystalline size and FWHM of ZnO thin films. The full width at half maximum (FWHM) values of the (100) peak values are 0.44, 0.97, 0.58 and 1.15° found at substrate bias voltages of 0, -30, -60, and -90 V respectively. In the investigation, the achieved FWHM value at unbiased condition is lower than the reported RF magnetron sputtered ZnO films prepared at substrate temperature of 200 °C [22]. The crystallite size (L) of the ZnO films has been calculated by using the Debye-Scherrer's equation [23].

$$L = 0.9\lambda/\beta\cos\theta \quad (1)$$

where β is the full width at half maximum of the peak and θ the Bragg diffraction angle. The crystallite size of the ZnO films formed at unbiased condition was 21 nm. The films deposited at -30 V the crystallite size was found to be 9.4 nm. Further increasing the bias voltage from -60 to -90 V the crystallite size of the films first increase and decreased as shown in Fig. 3.

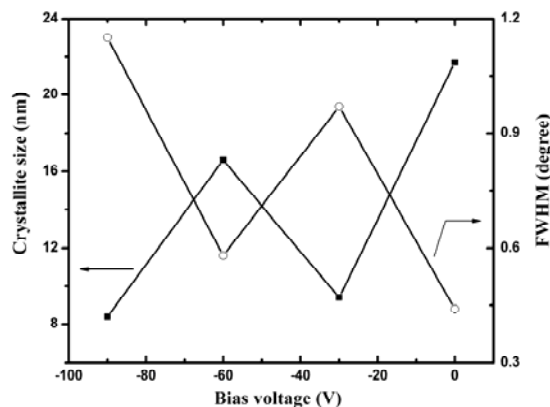


Fig.3. Crystallite size and FWHM of ZnO films deposited at different substrate bias voltages

Fig.4 shows the substrate bias voltage dependence dislocation density and strain of ZnO films. Dislocation density (δ) and strain (ϵ) were calculated by using the equations [24]

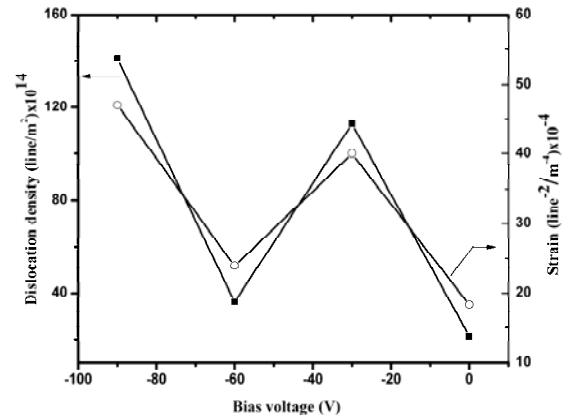


Fig. 4. Dislocation density and strain of ZnO films deposited at different substrate bias voltage

Dislocation density

$$(\delta) = 1/L^2 \quad (2)$$

Strain

$$(\epsilon) = \beta\cos\theta/4 \quad (3)$$

The obtained dislocation density values are 21, 113, 36, 141×10^{14} lines/m² and strain values are 18, 40, 23 and 47×10^{-4} line⁻²/m⁻⁴ respectively for substrate bias voltages of 0, -30, -60 and -90 V. The minimum value of the strain found at bias voltage of -60 V, due to the narrow line width, the ad-atom mobility also increases as the substrate bias increases which also results in the crystallite size and crystallinity of the film.

3.3. Surface morphology

3.3.1. SEM analysis

Fig.5 shows the scanning electron microscope (SEM) images of ZnO films formed at different substrate bias voltages. The films deposited at unbiased condition shows the porous like structures. When the films deposited at bias voltage of -30 V, exhibited the nanowires like structures. Further increasing the bias voltage to -60 V the number of nanowires decreased, and the size of the wires increased growth perpendicular to the films surface due to improvement of (002) c- axis orientation. At higher bias voltage of -90 V irregular shapes of nanowires were formed.

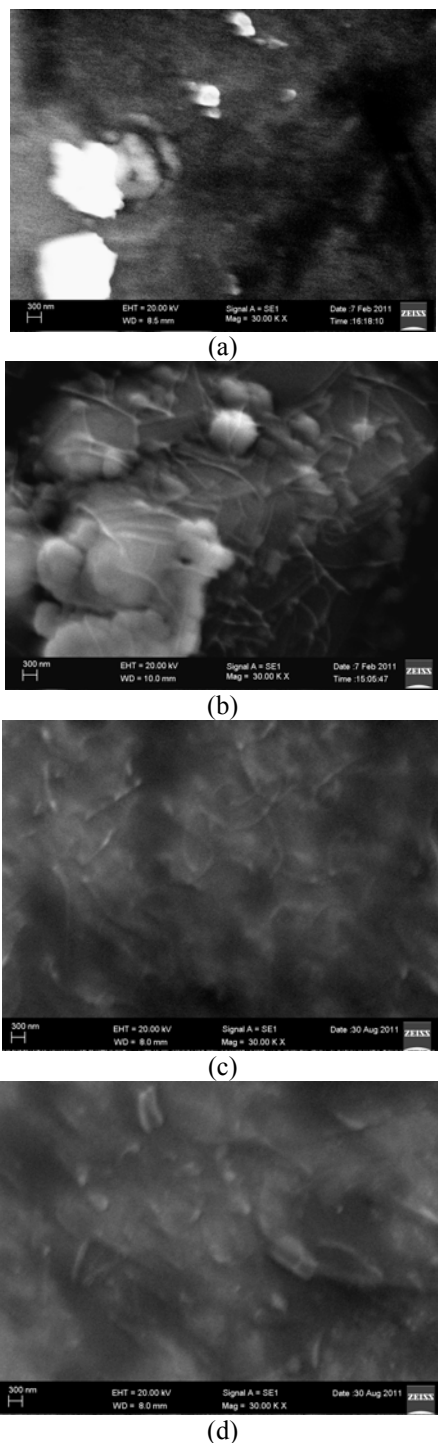


Fig.5. SEM images of ZnO films formed at different substrate bias voltages: (a) 0V (b) -30V (c) -60V and (d) -90 V

3.3.2. AFM analysis

Fig. 6 shows the atomic force micrographs of ZnO films deposited at different bias voltages ranging for 0 to -90 V. AFM images showed the difference in nanostructure according with variations of the XRD and SEM results. The films formed at substrate bias voltage of 0 V, the RMS roughness was 7.4 nm. As the increasing of bias voltage of -30 V the RMS roughness was increased to 14.1

nm. Further increase in the bias voltage to -90 V the roughness was decreased to 5.7 nm. Daniel et al. [25] reported a high RMS roughness of 58 nm in as-deposited and low RMS roughness of 1.5 nm in the films annealed at 673K in RF magnetron sputtered ZnO films.

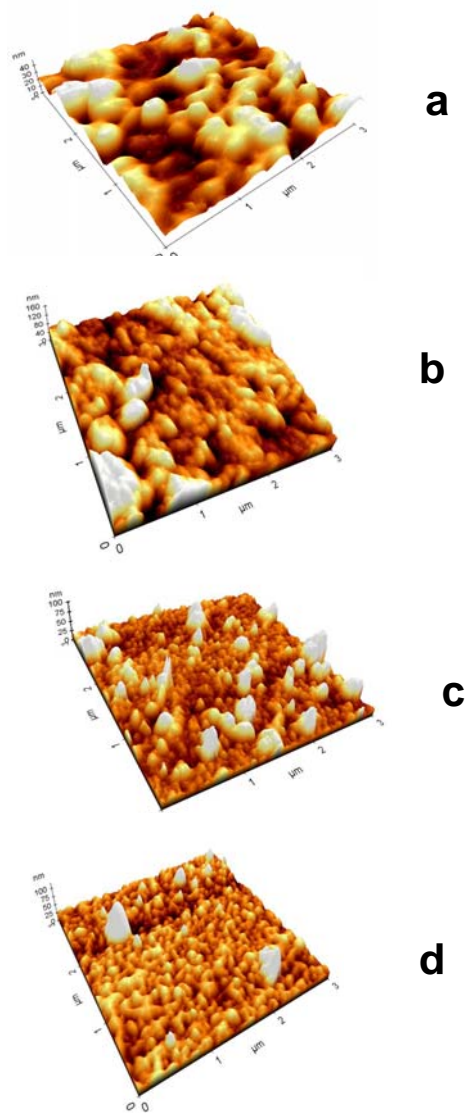


Fig.6. AFM images of ZnO films: (a) 0 V, (b) -30 V, (c) -60 V and (d) -90 V.

3.4. FTIR analysis

Fig.7 shows the Fourier transform infrared spectra of ZnO films deposited at different bias voltages. The FTIR spectra confirms the absorption peak of Zn-O bonding surrounding Zn atoms located at 413 cm^{-1} films deposited at 0 V bias condition. Nandi et al. reported [26] the absorption band at 409 cm^{-1} corresponds to Zn-O stretching vibration for a tetrahedral surrounding of Zn atoms. The FWHM of absorption peak minimum value found at -60 V bias voltage condition deposited sample, this results coincide with XRD results.

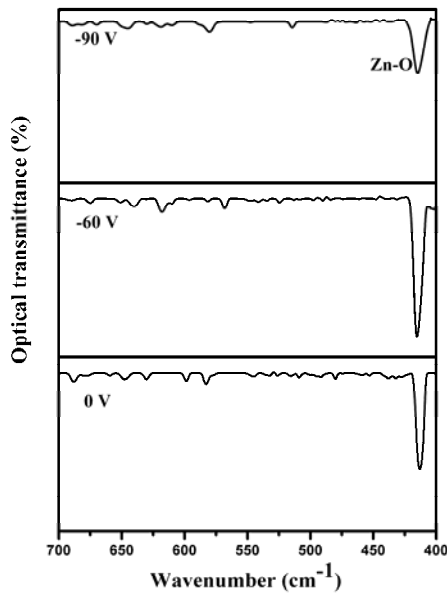


Fig.7. FTIR spectra of ZnO films formed at different substrate bias voltages.

The films deposited at bias voltage of -90 V the FWHM of absorption peak increased.

3.5. Optical properties

Fig.8 shows the optical transmittance spectra of the ZnO films deposited at different bias voltages of 0, -30, and -60 and -90 V. The transmittance is 95% at an un bias condition. With increase of bias voltage to -60 V the transmittance increased to 97%. Beyond this bias voltage the transmittance decreased. This reduction of transmittance in this higher bias condition due to the interstitial oxygen atoms in non stoichiometric oxygen rich ZnO films will cause to scatter and absorb the incident light.

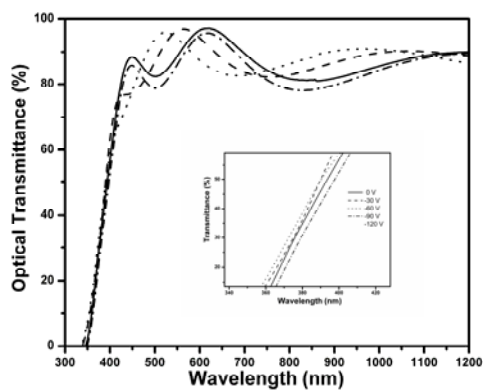


Fig.8. Optical transmittance spectra of ZnO films formed at different substrate bias voltages

Reddy et al. [27] reported DC sputtered copper oxide films optical transmittance decreases with increase of bias voltage. The average transmittance is about 88 % in the wavelength range from 450 to 650 nm.

Hoon et al. [28] observed that the transmittance of the films varies from 60 to 90% ($\lambda = 400$ to 850 nm) with the increase of substrate temperature from 27 to 400 °C in DC magnetron sputtered ZnO films.

Fig.9 shows the plot of $(\alpha h\nu)$ versus $(\alpha h\nu)^2$ of ZnO films formed different bias voltages ranging from 0 to -90 V. The optical band gap (E_g) can be calculated from the equation (2).

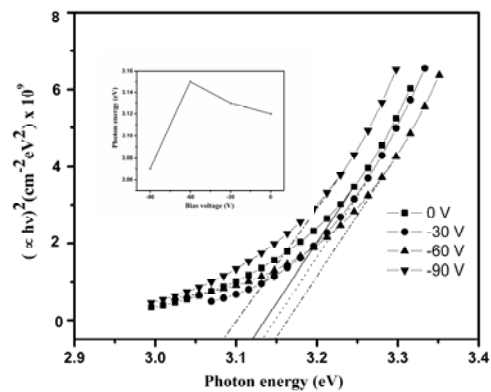


Fig.9. Plots of $(\alpha h\nu)^2$ vs photon energy ($h\nu$) of ZnO films formed at different substrate bias voltage

$$\alpha = (1/d) \ln T \quad (4)$$

where d is the film thickness, T the optical transmittance. The optical band gap (E_g) of the films were determined from the Tauc's relation [29]

$$\alpha h\nu \propto (h\nu - E_g)^m \quad (5)$$

where $m = 1/2$ for the direct transition.

The optical band gap of the ZnO films increased from 3.14 to 3.16 eV with increase of substrate bias voltage from 0 to -60 V. At higher substrate bias voltage of -90 V the optical band gap of the films decreased to 3.10 eV.

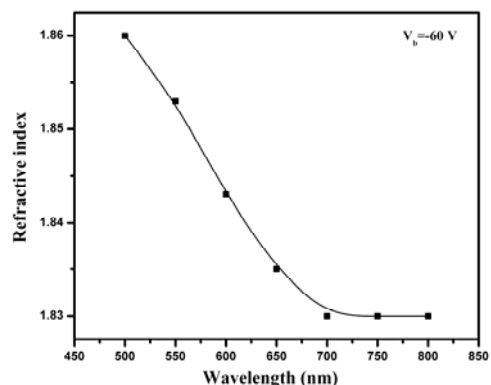


Fig.10. Variation of refractive index with wavelength of ZnO film formed at substrate bias voltage of -60 V

The refractive index (n) of the films was determined from the optical transmittance interference data employing Swanepoel's envelope method [30]

$$n(\lambda) = [N + (N^2 - n_0^2 n_1^2)^{1/2}]^{1/2} \quad (6)$$

and

$$N = 2n_0 n_1 [(T_M - T_m)/T_M T_m] + (n_0^2 + n_1^2)^{1/2} \quad (7)$$

where T_M and T_m are the optical transmittance maxima and minima respectively. The variation of refractive index with wavelength of the film formed at substrate bias voltage of -60 V is shown in Fig.10. Refractive index of the films decreased with the increase of wavelength. The refractive index decreased from 1.86 to 1.83 with increase of wavelength 500 to 700 nm and remains almost constant at higher wavelengths.

4. Conclusion

In this conclusion, the substrate bias voltage influenced structural, morphological and optical properties of ZnO films deposited onto p-type (100) silicon and glass substrates by using RF magnetron sputtering systematically investigated. The c- axis orientation of (002) peak was presence at bias voltage of -30 V. The maximum intensity of c- axis orientation of (002) phase found at bias voltage of -60 V. Fourier transform infrared spectroscopic studies confirms the presence Zn-O bonding at wavenumber of 413 cm^{-1} . The AFM analysis reveals the RMS roughness first increased and then decreased with increase of substrate bias voltage. The average optical transmittance of 88% was found at wavelength range from 450 to 650 nm. The optical band gap increased from 3.14 to 3.16 eV when the substrate bias voltage increased from unbiased to -60 V and then decreased to 3.10 eV at higher substrate bias voltage of -90 V. The refractive index of ZnO films was decreased from 1.86 to 1.83 with increase of wavelength from 450 to 700 nm at substrate bias voltage of -60 V.

References

- [1] R. Hong, H. Wen, C. Liu, J. Chen, J. Liao, J. Cryst. Growth., **314**, 30 (2011).
- [2] S. J. Kang, Y. H. Joung, Appl. Surf. Sci., **253**, 7330 (2007).
- [3] S. Manjunatha, L. S. Panchakarla, K. Biswas C. N. R. Rao, Inorg. chimica Acta, **63**, 2696 (2010).
- [4] M. Li, N. Choksi, R. L. Deleon, G. Tompa W. A. Anderson, Thin Solid Films, **515**, 7357 (2007).
- [5] A. Umar, Nanoscale Res. Lett., **4**, 1004 (2009).
- [6] Q. Wan and Q.H. Li, Appl. Phys. Lett., **84**, 3654 (2004).
- [7] R. A. Asman, G. Ferbmtier, F. Maily, P. G. Borrut, A. Foucoran, Thin Solid Films **473**, 49 (2005).
- [8] Z. Yin, N. Chen, R. Dai, L. Liu, X. Zhang, X. Wang, J. Lu and C. Chai, J. Cryst. Growth, **305**, 296 (2007).
- [9] S. Kitova and G. Danov, J. Phys: Conf. Series, **223**, 012022 (2010).
- [10] E. Senedim, H. Kavak and R Esen, J. Phys. Condens. Mater., **18**, 6391 (2006).
- [11] Y. Zhao, Y. Jiang and Y. Fang, J. Cryst. Growth, **307**, 278 (2007).
- [12] A. Y. Polykov, N. B. Smirnov, A. I. Belogorokhov, A. V. Govorkov A. Kozhukhova, J. Vac. Sci. Technol. B **25**, 1794 (2007).
- [13] C. C. Ting, C. H. Li, C. Y. Kuo, C. C. Hsu, Thin Solid Films, **518**, 4156 (2010).
- [14] Y. C. Lin, B. L. Wang, W. T. Yen, C. T. Ha, C. Peng, Thin Solid Films **518**, 4928 (2010).
- [15] X. C. Wang, X. M. Chen, B. H. Yang, J. Alloys. Compounds, **488**, 232 (2009).
- [16] Z. W. Yang, S. H. Han, T. L. Yang, L. Ye, D. H. Zhang, H. L. Ma, C. H. Chang, Thin Solid Films **366**, 4 (2000).
- [17] V. Nirupama, M. Chandra Sekhar, P. Radhika, B. Sreedhar, S. Uthanna, J. Optoelectron. Adv. Mater., **11**, 320 (2009).
- [18] A. Mallikharjuna Reddy, A. Sivasankar Reddy, P. Sreedhara Reddy, Mater. Chem. Phys., **125**, 434 (2011).
- [19] H. Ma, X. Hao, J. Ma, Y. Yang, S. Huang, F. Chen, D. Zhang, Surf. Coat. Technol., **161**, 58 (2002).
- [20] S. Flickyngerova, K. Shtereva, D. Hasko, I. Novotny, V. Tvarozek, P. Sutta, E. Vavrinsky, Appl. Surf. Sci., **254**, 3643 (2008).
- [21] M. C. Barnes, S. Kumar, L. Green, M. N. Wang, A. R. Gerson, Surf. Coat. Technol. **190**, 321 (2005).
- [22] S.J. Kang and Y.H. Young, Appl. Surf. Sci., **253**, 7330 (2007).
- [23] B. D. Cullity, Elements of X-ray Diffraction, 2nd Ed., Addison Wesley, London, 1978.
- [24] S. Lalita, R. Sathyamurthy, S. Senthilarasu, A. Subbarayan, K. Natarajan, Solar Energy Mater. Solar Cells, **82**, 187 (2004).
- [25] G. P. Daniel, V. B. Justinictor, P. B. Nair, K. Joy, P. Koshy, P. V. Thomas, Physica B, **405**, 1782 (2010).
- [26] S. K. Nandi, S. Chakraborty, M. K. Bera, C. K. Maiti, Bull. Mater. Sci. **30**, 247 (2007).
- [27] A. Sivasankar Reddy, G. Venkata Rao, S. Uthanna P. Sreedhara Reddy, Physica B, **370**, 29 (2005).
- [28] J. W. Hoon, K.Y. Chan, J. Krishnasamy, T.Y. Tou D. Knipp, Appl. Surf. Sci., **257**, 2515 (2011)]
- [29] C. F. Yu, C. W. sung, S. H. Chen, S. J. Sun, Appl. Surf. Sci., **256**, 792 (2009).
- [30] R. Swanepoel, J. Phys. E: Sci. Instrum., **16**, 1214 (1983).

*Corresponding author: uthanna@rediffmail.com